DOE/NASA/1011-78/25
NASA TM-78894

COLD-AIR PERFORMANCE OF THE COMPRESSOR-DRIVE TURBINE OF THE DEPARTMENT OF ENERGY BASELINE AUTOMOBILE GAS-TURBINE ENGINE

Richard J. Roelke and Kerry L. McLallin
National Aeronautics and Space Administration
Lewis Research Center

July 1978

Prepared for
U.S. DEPARTMENT OF ENERGY
Office of Conservation and Solar Applications
Division of Transporation Energy Conservation

DOE/NASA/1011-78/25
NASA TM-78894

COLD-AIR PERFORMANCE OF THE COMPRESSOR-DRIVE TURBINE OF THE DEPARTMENT OF ENERGY BASELINE AUTOMOBILE GAS-TURBINE ENGINE

Richard J. Roelke and Kerry L. McLallin
National Aeronautics and Space Administration
Lewis Research Center
Cleveland, Ohio 44135

July 1978

Prepared for
U. S. Department of Energy
Office of Conservation and Solar Applications
Division of Transportation Energy Conservation
Washington, D. C. 20545
Under Interagency Agreement EC-77-A-31-1011

COLD-AIR PERFORMANCE OF THE COMPRESSOR-DRIVE TURBINE OF THE DEPARTMENT OF ENERGY BASELINE AUTOMOBILE GAS-TURBINE ENGINE

by Richard J. Roelke and Kerry L. McLallin

Lewis Research Center

SUMMARY

The aerodynamic performance of the compressor-drive turbine and transition duct of the Department of Energy baseline automobile gas-turbine engine was determined. The tests were conducted with air as the working fluid at nominal, turbine-inlet, total conditions of 300 K and 0.69 bar. Mass flow, torque, speed, temperatures, and pressures were measured to determine turbine performance. Static pressures were measured in the transition duct located immediately behind the turbine to assess the diffusion process.

Along the turbine operating line, the total efficiency varied from 0.824 at design power to just under 0.80 at intermediate power. At low power the efficiency was 0.81 and there was a small static-pressure rise across the rotor hub. Although the effect of this pressure rise on rotor losses was not determined, it is probably small. The transition duct diffused the air without any signs of flow separation. At design power, the pressure recovery was 0.523 and the effectiveness was 0.666.

INTRODUCTION

The Department of Energy (DOE) is continuing the program started by the Energy Research and Development Administration (ERDA) to demonstrate a gas-turbine-powered automobile that meets the 1978 Federal Emission Standards with acceleration characteristics and fuel economy that are competitive with those of spark-ignition-engine-powered automobiles. Part of this program, as defined by ERDA, consists of establishing a baseline for automobile turbomachinery performance. By competitive bidding, ERDA selected Chrysler Corporation's sixth-generation, prototype, gas-turbine engine as the baseline engine. Turbomachinery components from this engine were obtained by ERDA and furnished to NASA for testing. The Lewis Research Center, under an interagency agreement, was given the responsibility for evaluating the aerodynamic performance of the components. The aerodynamic performance of the power turbine is reported in reference 1. This report evaluates the aerodynamic performance of the compressor-drive turbine and the downstream transition duct.

The compressor-drive turbine is a 14-centimeter-tip-diameter, single-stage, axial-flow machine. At full engine power (112.5 kW) the turbine design specific work is 2.046×10^5 joules per kilogram and the gas flow is 1.015 kilograms per second. The turbine work factor at full engine power is 2.45, a result that indicates a moderately high aerodynamic loading. In the engine, the transition duct, an annular diffusing duct 6.8 centimeters long, is located between the compressor-drive and power turbines.

The performance of the turbine and the downstream transition duct was determined with air at nominal turbine-inlet total conditions of 300 K and 0.69 bar and at total- to static-pressure ratios from 1.2 to 5.0 and speeds from 50 to 110 percent of equivalent design speed. Rotor-exit radial surveys of angle, total pressure, and total temperature were taken at nominal equivalent design speeds of 50 and 100 percent and at pressure ratios corresponding to low- and design-power operating points. Static pressures were measured on either side of each blade row and along the inner and outer walls of the transition duct.

The aerodynamic performance of the turbine is presented herein in terms of equivalent mass flow, torque, specific work, and efficiency. The aerodynamic performance of the transition duct is evaluated in terms of pressure recovery and effectiveness at two operating conditions. Also included are descriptions of the compressor-drive turbine, the test facility, and the procedures used in the evaluation.

SYMBOLS

b	blade height, cm
C_p	diffuser pressure recovery, $(p_7 - p_6)/(p_6' - p_6)$
c	chord, cm
Δh	specific work, J/kg
L	dimension of transition duct (fig. 4(b))
l	distance to pressure tap (fig. 4(b))
m	mass flow, kg/s
p	pressure, bars abs
r	radius, cm

s pitch, cm

T absolute temperature, K

U blade velocity, m/s

V absolute gas velocity, m/s

W relative gas velocity, m/s

α absolute gas flow angle measured from axial direction, deg

γ ratio of specific heats

δ ratio of inlet total pressure to U.S. standard sea-level pressure, $p'_{4.5}/p^*$

ϵ function of γ used in relative parameters to those using air inlet conditions at U.S. standard sea-level conditions, $(0.740/\gamma)[(\gamma + 1)/2]^{\gamma/(\gamma-1)}$

η' total efficiency (based on ratio of inlet to exit total pressures)

θ_{cr} squared ratio of critical velocity at turbine inlet to critical velocity at U.S. standard sea-level conditions, $(V_{4.5}/V^*_{cr})^2$

μ viscosity, $(N \cdot s)/m^2$

ξ diffuser effectiveness, $C_p/C_{p,i}$

τ torque, $N \cdot m$

ω turbine speed, rad/s

Subscripts:

cr conditions at Mach 1

h hub section

i ideal

m mean section

max maximum

t tip section

te trailing edge

u tangential component

4.5 station at manifold inlet (fig. 2)

5 station at stator inlet (fig. 2)

5.5 station at stator exit (fig. 2)

6 station at rotor exit (fig. 2)

7 station at transition-duct exit (fig. 2)

Superscripts:

' absolute total state

* standard

TURBINE DESCRIPTION

Shown in figure 1 is a cross section of the baseline gas-turbine engine. In this view, air enters at the left, is compressed by the compressor, picks up heat in the regenerators, and then enters the combustor (not shown in the figure). After leaving the combustor, the hot gas is expanded in the compressor-drive and power turbines in series, passes through the hot side of the regenerators, and is exhausted from the engine. Useful power from the engine is delivered through a reduction gear attached to the power turbine. The compressor-drive turbine and the transition duct are the subjects of this report.

A cross section of the compressor-drive turbine is shown in figure 2. The turbine is a single-stage, axial-flow machine. Combustion gases enter the inlet vortex manifold through a tangential entry port and are then accelerated axially into the nozzle. The manifold flow area is largest at the entry port and decreases around the periphery. Because of the swirl set up by the vortex manifold, the nozzle does very little additional turning of the flow; for example, the turning is 20.4° at the mean radius. The exit flow angle at the mean radius is 65.4°. Because of the small amount the flow is turned in the nozzle and the large exit angle, there is a very short guided channel between adjacent stator blades. These features are shown by the blading mean sections in figure 3. Selected stator aerodynamic parameters are listed in table I.

The rotor is welded to the shaft, which in turn is mounted in two sleeve bearings. The rotor is unshrouded and the tips of the blades are approximately alined with the inside diameter of the stator shroud (fig. 2). The radial clearance between the rotor and the nozzle shroud overhang is 0.254 millimeter, or 1.7 percent of the blade height. The camber angles are approximately 105°, 99°, and 95° at the hub, mean, and tip, respectively. Additional aerodynamic parameters are listed in table I.

The transition duct is located between the compressor-drive and power turbines. Three struts in the flow passage support the inner body. The struts have a streamlined shape and are generally alined to the flow. The angle of the flow entering the transition duct does not vary appreciably along the engine operating line as is shown in the section Rotor exit flow angle.

The turbine requirements for two engine operating conditions are given in table II. The low- and design-power conditions represent the limits of the normal turbine operating range. Good turbine performance is equally important at both design and low power.

In an automotive application, the engine is operated at low power most of the time, and this type of operation has a significant impact on the overall fuel economy of the engine. However, design-point (full power) performance must not be unduly compromised or the engine will become too large for a given design output. Comparing the work factors $\Delta h/U_m^2$ for the two engine conditions shows that the turbine operates with a nearly constant work factor over a wide range of conditions.

APPARATUS AND INSTRUMENTATION

The test apparatus included the turbine, an airbrake dynamometer, and an inlet and exhaust piping system. The turbine was tested with air at nominal inlet conditions of 300 K and 0.69 bar. During operation, air from the laboratory high-pressure-air system flowed through the inlet piping, a calibrated flat-plate orifice, and an automatic pressure control valve and into the test unit. After expanding through the turbine, the air was discharged through an exhaust-line control valve to the laboratory low-pressure exhaust system. The turbine pressure ratio was set by keeping the inlet pressure constant and varying the exhaust pressure.

The airbrake dynamometer was used to absorb the turbine power as well as to control the speed. The reaction torque of the dynamometer, which floats on a thin film of pressurized air, was measured with a load-cell transducer. Speed was measured with a shaft-mounted gear, a magnetic pickup, and an electronic pulse counter.

The instrumentation stations are shown in figure 2. The number, type, and location of measurements at each station are shown in figure 4. At station 4.5 (manifold inlet) the instrumentation consisted of four wall static-pressure taps, four internally beveled total-pressure probes, and four thermocouples. At station 5 (stator inlet), approximately 4.4 millimeters (three-tenths of the mean-diameter axial chord) upstream of the stator leading edge, the instrumentation consisted of three fixed-angle, total-pressure probes at the annulus mean radius and three inner-wall and three outer-wall static-pressure taps. At station 5.5 (stator exit) the instrumentation consisted of three inner-wall and three outer-wall static-pressure taps. At station 6 (rotor exit), approximately 1 chord length downstream of the rotor trailing edge, the instrumentation consisted of three combination probes and three inner-wall and three outer-wall static-pressure taps. The combination probes were mounted in actuators that permitted automatic self-alinement to the gas flow direction and remotely controlled radial translation. These probes measured total temperature, total pressure, and flow angle. During the performance tests, the probes were positioned at the annulus mean radius. The self-alining probes were also used to obtain the radial gradients of rotor-exit total pressure, total temperature, and flow angle at equivalent design speed and a total-pressure ratio of 2.20 and at 51 percent of equivalent design speed and a total pressure ratio of 1.31.

In the transition duct (fig. 4(b)) the instrumentation consisted of static-pressure taps on the end walls. Between stations 6 and 7, nine static-pressure taps were installed on the inner wall and nine on the outer wall. At station 7 an additional six static-pressure taps were installed. All static-pressure taps in the turbine and the transition duct were 0.51 millimeter in diameter.

All data were recorded on an integrating, digital, data-recording system. A digital computer processed the data.

TEST PROCEDURE AND DATA REDUCTION

The turbine was operated at nominal inlet conditions of 0.69 bar absolute and 300 K. These conditions correspond to a Reynolds number ($Re = m/\mu r_m$) of about 320 000 at equivalent design speed and pressure ratio. They were selected to give a test Reynolds number that would be close to the Reynolds number (330 000) at the design engine condition. Data were taken for equivalent inlet-total- to exit-tip-static-pressure ratios $p'_{4.5}/p_{6,t}$ from about 1.2 to 5.0 and speeds from 50 to 110 percent of equivalent design speed.

At equivalent design speed and an inlet-total- to exit-total-pressure ratio $p'_{4.5}/p'_6$ of 2.20 and at 51 percent of design speed and a $p'_{4.5}/p'_6$ of 1.31, survey data were taken at station 6 with the combination probes at each of 11 radial positions between the hub and the tip. These operating conditions represent the nominal range of turbine operation in the engine. The actuated probes were positioned at the mean radius for all other turbine tests.

The turbine tare torque was determined by motoring the test unit, with a bladeless rotor installed, over the range of test speeds. A tare torque of approximately 0.067 newton meter, or 5.7 percent of the turbine output, was measured at equivalent design speed and pressure ratio.

The turbine specific work was calculated from weight-flow, speed, and torque measurements. The torque value used was the sum of the torque indicated by the load cell and the tare torque. The overall aerodynamic performance of the turbine was based on the total conditions measured at the vortex-manifold inlet (station 4.5) and the rotor-exit mean radius (station 6). The stage total-pressure ratios so obtained were adjusted to agree with the averaged total-pressure ratios obtained from the two turbine-exit surveys. Thus, any pressure loss in the vortex manifold is included in the turbine performance.

RESULTS AND DISCUSSION

This section presents the overall aerodynamic performance of the turbine blading and transition duct. Internal flow characteristics are given in terms of end-wall static pressures and rotor-exit surveys of total pressure, total temperature, and absolute flow angle; and the transition-duct performance is given in terms of static-pressure rise and effectiveness. The basic quantities measured (i. e., weight flow, torque, pressures, and flow angles) are presented as functions of the inlet-total- to exit-tip-static-pressure ratio $p'_{4.5}/p_{6,t}$. The experimental correspondence between this pressure ratio, which was used to set the turbine expansion during the tests, and the inlet-total- to exit-total-pressure ratio $p'_{4.5}/p'_6$ is shown by smoothed curves in figure 5. The ● symbols in the figure indicate the equivalent total-pressure ratios listed in table II. The overall performance map also is presented in terms of the total-pressure ratio.

Overall Aeronautics Performance

The turbine overall aerodynamic performance, which is based on measurements at stations 4.5 and 6, is presented in figures 6 to 8. The performance data were obtained with air at an inlet total temperature of 300 K and an inlet total pressure of 0.69 bar and were converted to equivalent parameters.

Mass flow. - The variation in equivalent mass flow with equivalent inlet-total- to exit-tip-static-pressure ratio for the equivalent test speeds is shown in figure 6. Choking flow was obtained for all speeds. For rotor speeds equal to or less than 100 percent of design, the stator choked before the rotor. At 110 percent of design speed the rotor choked at a slightly lower flow than the stator. The equivalent total-pressure ratio at design (table II) is 2.089. At this equivalent total-pressure ratio, the corresponding inlet-total- to exit-tip-static-pressure ratio is 2.99 (fig. 5). At this pressure ratio and at equivalent design speed, an equivalent mass flow of 0.558 kilogram per second was obtained (fig. 6), which is 1/2 percent less than the 0.561 kilogram per second listed in table II. However, the calculated thermal expansion of the test hardware between rig temperature and engine temperature would increase the flow areas by about 2 percent. Therefore, the component rig mass flow should be about 98 percent of 0.561 kilogram per second, or 0.550 kilogram per second. Therefore, the rig mass flow is about $1\frac{1}{2}$ percent larger than design.

Torque. - The variation of equivalent torque with the inlet-total- to exit-tip-static-pressure ratio for the equivalent test speeds is shown in figure 7. Turbine-limiting loading was approached at the higher pressure ratios for all speeds, as indicated by the slope of the torque curves approaching zero. At the inlet-total- to exit-tip-static-pressure ratio of 2.99 and at equivalent design speed, the measured equivalent torque was 11.30 newton meters, which is 4.4 percent lower than the torque (11.82 N·m) calculated from the power and speed listed in table II. The measured mass flow and torque can be used to indicate the change in tangential velocity ΔV_u across the stage. Calculating ΔV_u from test measurements and comparing it with the value obtained from the design conditions in table II indicate that the stage efficiency is some 4 percent lower than design and that the turbine must operate at a higher pressure ratio to produce the required work.

Performance map. - The performance map (fig. 8) was generated from the data of figures 5 to 7. At a given total-pressure ratio, and for each speed, smooth-curve values of torque and weight flow were used to calculate the equivalent specific work $\Delta h/\theta_{cr}$, the mass-flow speed parameter $m\epsilon\omega/\delta$, and the total efficiency η'. Superimposed on the map is the turbine operating line when the turbine is installed in the engine.

The turbine attained efficiencies (fig. 8) from 0.85 to just under 0.70 for the range of test conditions. At the equivalent design specific work of 47 233 joules per kilogram and at equivalent design speed, denoted by the ■ symbol, the turbine efficiency was 0.824, which is 0.036 less than the design efficiency of 0.86 calculated from the conditions given in table II. The equivalent specific work of 47 233 joules per kilogram was obtained at a total-pressure ratio of 2.166 rather than the design value of 2.089. Traversing the engine operating line shows that the efficiency changed only about 0.025, from 0.824 at design power to about 0.80 at 70 percent of equivalent design speed and an equivalent total-pressure ratio of 1.5. At the low-power condition, denoted by the ▲ symbol, the turbine efficiency was 0.81, which is 0.05 more than the corresponding low-power efficiency of 0.76 calculated for the conditions in table II. As shown in table II, the work factor at the low-power condition was only slightly higher than at design. This difference can account for about 0.004 of the efficiency difference, 0.014, between the design and low-power conditions. The remaining 1-point difference was probably due to changes in rotor incidence and reaction between the two operating conditions. These changes are discussed in the following sections. At the low-power operating condition, the equivalent specific work of 16 030 joules per kilogram was obtained at a total-pressure ratio of 1.28.

Turbine Flow Conditions

The hub and tip static pressures measured at stations 5, 5.5, and 6 and the mean-radius flow angles measured at station 6 are plotted in figures 9 and 10. These measurements were used to indicate the flow conditions in the turbine.

Static-pressure distribution. - The static-pressure distribution through the turbine is shown in figure 9 as a function of inlet-total- to exit-tip-static-pressure ratio for 56.5 and 100 percent of equivalent design speed. Stations 5, 5.5, and 6 are the stator inlet, the stator exit, and the rotor exit, respectively. These stations are shown in figure 2. All pressures were ratioed to the mean-radius inlet total pressure p_5'.

At low power (specific work of 16 030 J/kg and 56.5 percent of equivalent design speed), the turbine inlet-total- to exit-tip-static pressure ratio $p_{4.5}'/p_{6,t}$ was approximately 1.39 (dashed line in fig. 9(a)). At this turbine pressure ratio and up to a ratio of 2.0, there was a small static-pressure rise across the rotor hub, which may have increased the aerodynamic losses at this operating condition. For all turbine pressure ratios at equivalent design speed (fig. 9(b)), there was positive reaction across both blade rows. The inlet-total- to exit-tip-static pressure ratio of 3.32 (corresponding to the design specific work of 47 233 J/kg) is shown by a dashed line.

Rotor-exit flow angle. - The mean-radius flow angles at the rotor exit are shown in figure 10 as a function of the inlet-total- to exit-tip-static-pressure ratio for all test speeds. The angles plotted were the numerical averages of the three angles measured by the self-alining probes. Positive angles, as measured from the axial direction, indicate that the exit swirl was in the direction of rotor rotation.

At each speed the exit angle decreased with increasing pressure ratio until a minimum was reached. At lower speeds, the angle increased slightly after the maximum negative value was reached. This may be caused by a greater increase in the axial velocity component than in the tangential velocity component as turbine-limiting loading was approached. Limiting loading was more nearly approached at these low speeds (as shown in fig. 7) than at higher speeds. The turbine operating line during engine operation is superimposed on figure 10. The symbols shown at either end of the operating line, at pressure ratios of 1.39 and 3.32, represent the match points for the low and design specific works, respectively. The mean-radius exit angle at the low specific work was 13° and that at the design specific work was -23.5°. Therefore, the mean-radius, rotor-exit flow angle varied about 10.5° along the entire turbine operating line. However, the variation over the entire annulus was greater, as indicated by radial surveys.

Turbine-Exit Radial Surveys

The results of radial surveys (station 6) of total pressure, absolute flow angle, and temperature at two turbine operating conditions are shown in figures 11 and 12. The operating conditions surveyed were (1) equivalent design speed at an inlet-total- to exit-total-pressure ratio $p_{4.5}'/p_6'$ of 2.20 and (2) nominal 50 percent of equivalent design speed at a $p_{4.5}'/p_6'$ of 1.31. These operating conditions were near the design and low-power conditions listed in table II.

Flow angle. - The variation in flow angle for the two operating conditions is shown in figure 11. The measurements of each of the three combination probes are shown, along with the average. (The circumferential locations of the probes are shown in fig. 4(a).) There was considerable variation in the flow angle both circumferentially and radially. The largest circumferential variation among the three probes occurred at 40 percent of blade span and again at the tip. At design speed (fig. 11(a)) the flow was turned considerably more near the hub than over the rest of the blade span. At low power (fig. 11(b)) the measured angles showed many of the same characteristics as the design speed survey: The flow was turned much more at the hub than elsewhere. At the midspan there was a region of low turning, which could be caused by a secondary flow core in the flow stream or by flow separation off the rotor suction surface.

Total-temperature and total-pressure surveys. - The total-temperature and total-pressure variations measured at the turbine exit are presented in figure 12. The measurements of the three probes were plotted individually, but frequently the values at any given radius were identical, which indicates very little circumferential variation. The radial variation in temperature and pressure was greater at equivalent design speed (fig. 12(a)) than at 50 percent of equivalent design speed (fig. 12(b)). The stage specific work at equivalent design speed was calculated from the survey-indicated gas temperatures and found to be approximately 7 percent lower than that calculated from torque, weight flow, and speed. It is believed that the survey-indicated gas temperatures were probably in error. Since, as already stated, the test inlet temperature was 300 K, the exhaust temperature was about 255 K. Most of the thermocouple probe extended from the test rig and was surrounded by air at about 305 K. As the probes were moved radially outward (higher percent of blade span), increased heat flow toward the thermocouple probably caused errors in the gas temperature measurement.

Transition Duct

The static pressures measured in the transition duct between the compressor-drive and power turbines are shown in figure 13. The static pressures are shown along the inner and outer walls for two turbine operating conditions. The static pressure gradually increased along the length of the duct. The pressure recovery coefficient ($C_p = (p_7 - p_6)/(p_6' - p_6)$) within the duct was 0.523 at design power and 0.542 at low power. The corresponding effectiveness values ($\xi = C_p/C_{p,i}$) were 0.666 and 0.767. According to Sovran and Klomp (ref. 2), the subject transition duct has optimum diffuser geometry and an indicated pressure recovery coefficient (with uniform inlet flow and thin boundary layers) of about 0.6. They state that thick inlet boundary layers and/or nonuniformity of inlet velocity profiles will reduce the pressure recovery. Therefore, the transition duct appeared to have performed quite satisfactorily.

SUMMARY OF RESULTS

The aerodynamic performance of the compressor-drive turbine of the Department of Energy baseline automobile gas-turbine engine, manufactured by the Chrysler Corporation was determined with air at nominal conditions of 300 K and 0.69 bar. Speed was varied from 50 to 110 percent of equivalent design speed for equivalent total- to static-pressure ratios from 1.2 to 5.0. In addition, static pressures were measured in a transition duct between the compressor-drive and power turbines to determine the effectiveness of the diffusion process in that component. The results of the investigation are as follows:

1. The turbine total efficiency along its engine operating line varied from 0.824 at design engine power to just under 0.80 at 70 percent of equivalent design speed. At the low end of the operating line (56.5 percent of equivalent design speed) the turbine efficiency was 0.81.

2. Static pressures measured at the hub and tip end walls indicated that there was positive rotor reaction at design engine power but a small amount of negative reaction at the low end of the operating line. This negative reaction may have slightly increased the rotor aerodynamic losses.

3. Turbine-exit radial surveys of angle, temperature, and pressure showed that circumferential variations were considerable in flow angle but slight in temperature and pressure. The data also showed considerably more turning of the flow in the hub region than in the region from blade midspan to tip.

4. The transition duct diffused the air well with no signs of flow separation off the walls. At design conditions, the pressure recovery was 0.523 and the effectiveness was 0.666.

Lewis Research Center,
National Aeronautics and Space Administration,
Cleveland, Ohio, March 21, 1978,
778-32.

REFERENCES

1. Kofskey, Milton G.; and Nusbaum, William J.: Cold-Air Performance of a Free-Power Turbine Designed for a 112-Kilowatt Automotive Gas-Turbine Engine. I - Design Stator-Vane-Chord Setting Angle of 35°. NASA TP-1007; DOE Report CONS/1011-12, 1978.

2. Sovran, Gino; and Klomp, Edward D.: Experimentally Determined Optimum Geometries for Rectilinear Diffuser with Rectangular, Conical or Annular Cross-Section. Fluid Mechanics of Internal Flow, Proceedings of a Symposium, Warren, Michigan, Sept. 20-21, 1965, Gino Sovran, ed., Elsevier Publishing Co. (Amsterdam), 1967, pp. 270-312.

TABLE I. - TURBINE BLADING PARAMETERS

Blade row	Aspect ratio, b/c_m	Blade height, b, cm	Number of blades	Solidity, c/s	
Stator	0.547	1.52	19	Hub	1.471
				Mean	1.356
				Tip	1.243
Rotor	1.138	1.52	53	Hub	2.110
				Mean	1.817
				Tip	1.618

TABLE II. - TURBINE OPERATING PARAMETERS

	Low engine power (7.1 kW)		Design engine power (112.5 kW)	
	Engine	Equivalent	Engine	Equivalent
Inlet temperature, K	1050.6	288.15	1283.1	288.15
Inlet pressure, bar	1.522	1.013	3.959	1.013
Turbine power, kW	20.23	7.36	207.67	26.50
Mass flow, kg/s	0.354	0.459	1.015	0.561
Rotative speed, rad/s	2395.7	1269.2	4671.5	2244.7
Specific work, J/kg	5.71×10^4	1.603×10^4	2.046×10^5	4.723×10^4
Total-pressure ratio, $p'_{4.5}/p'_6$	1.293	[a]1.303	2.020	[a]2.089
Work factor, $\Delta h/U_m^2$	2.60	2.60	2.45	2.45
Total efficiency	0.76	0.76	0.86	0.86

[a]The equivalent pressure ratio differs from the engine pressure ratio due to changes in gas properties between engine temperatures and equivalent temperature.

22877 rpm

44609 rpm

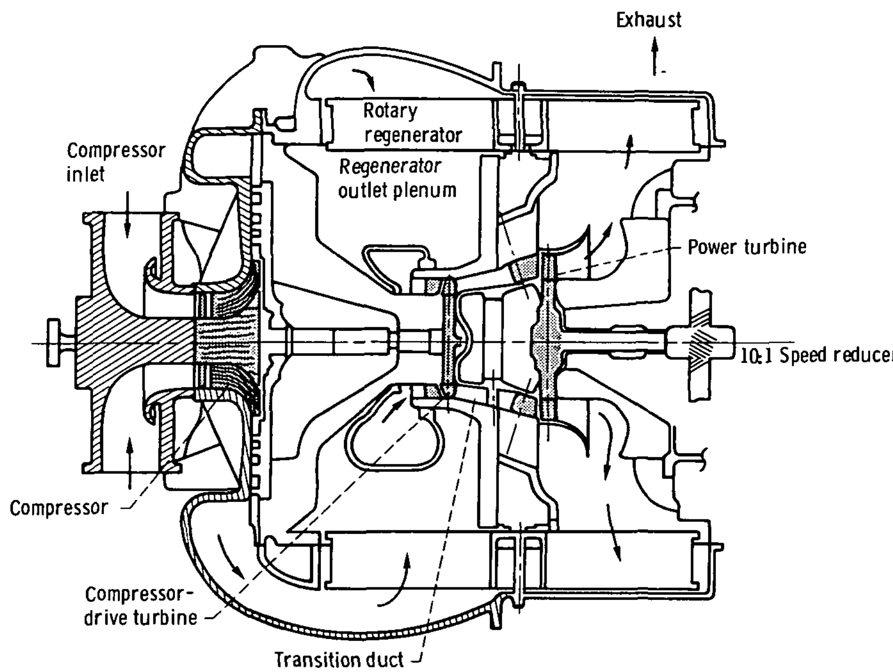

Figure 1. - DOE baseline automobile gas-turbine engine.

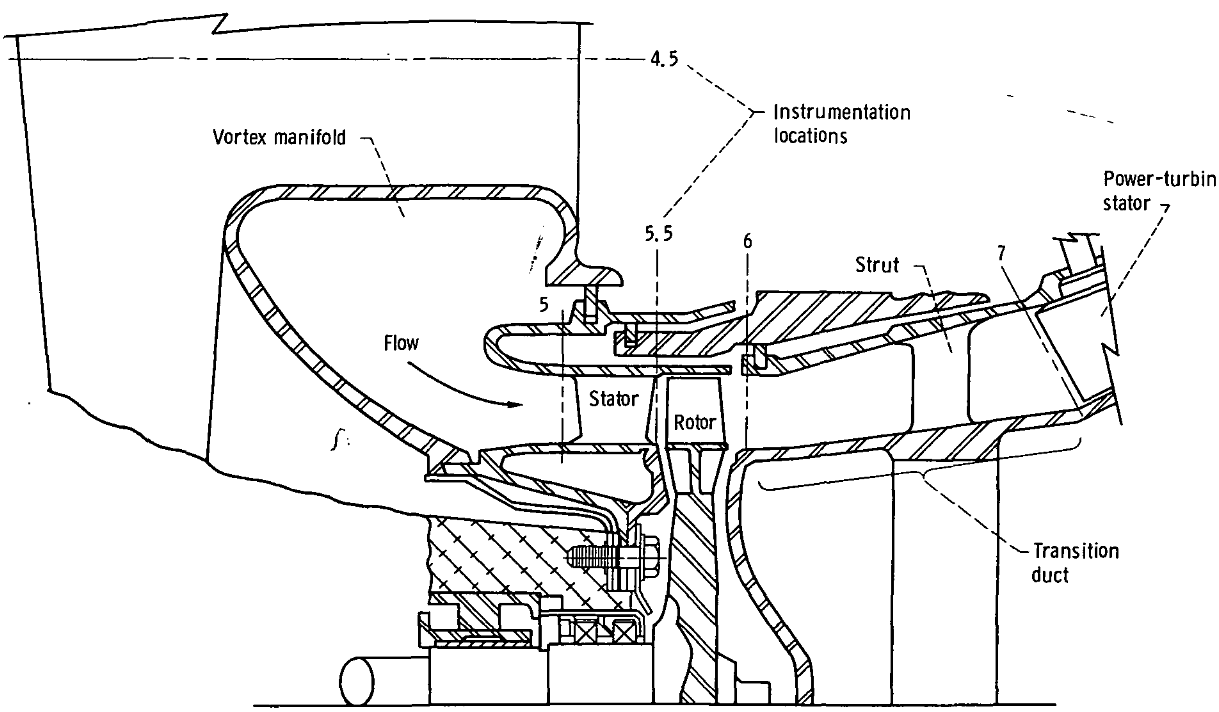

Figure 2. - Cross section of baseline compressor-drive turbine and transition duct.

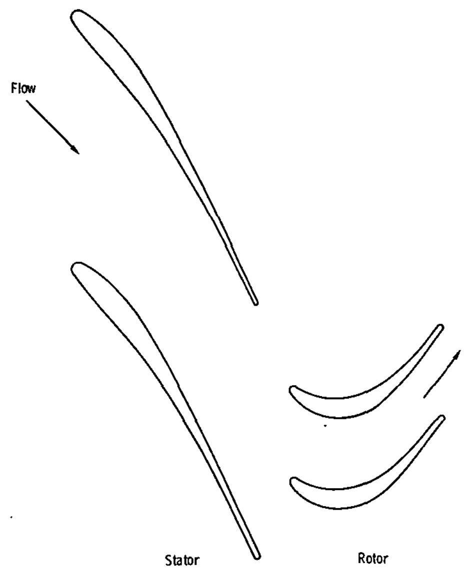

Figure 3. - Mean-radius blading profiles and flow passages.

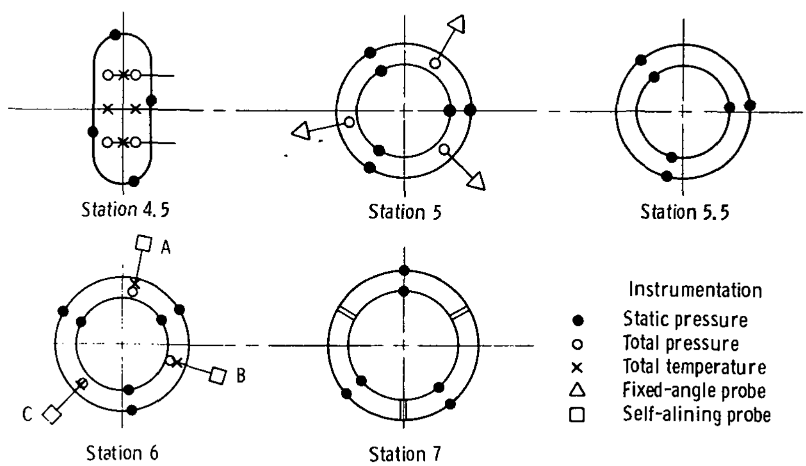

(a) Flow path measurements, viewed looking upstream.

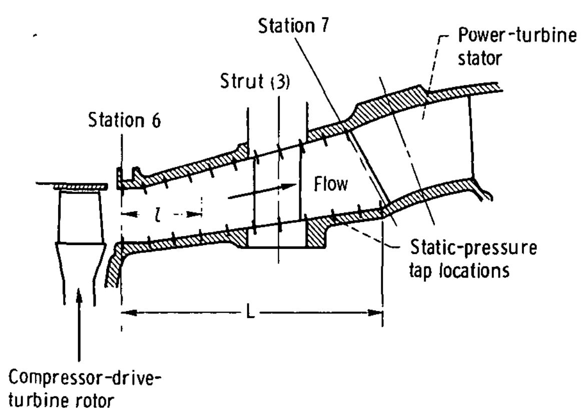

(b) Transition-duct static pressures.

Figure 4. - Test turbine instrumentation

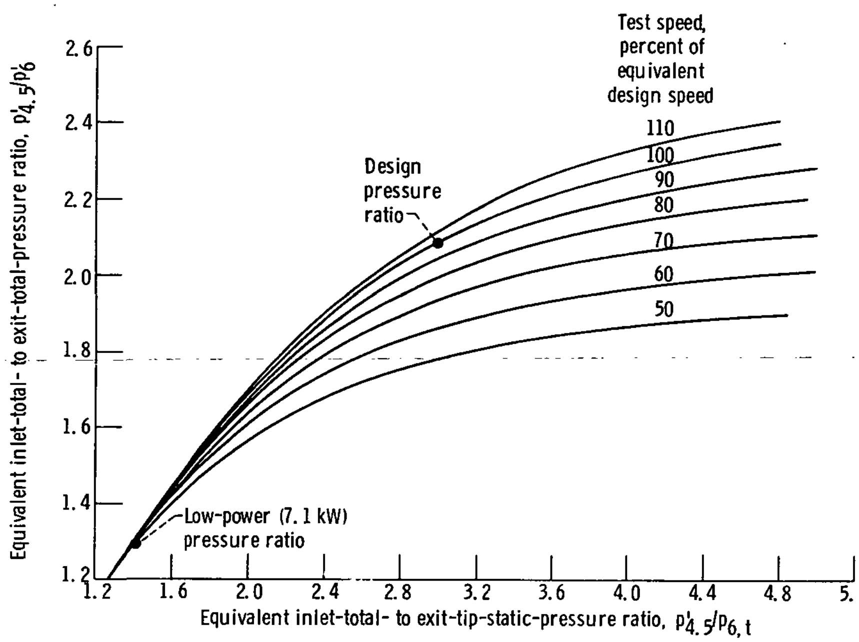

Figure 5. - Variation of total- to total-pressure ratio with total- to static-pressure ratio.

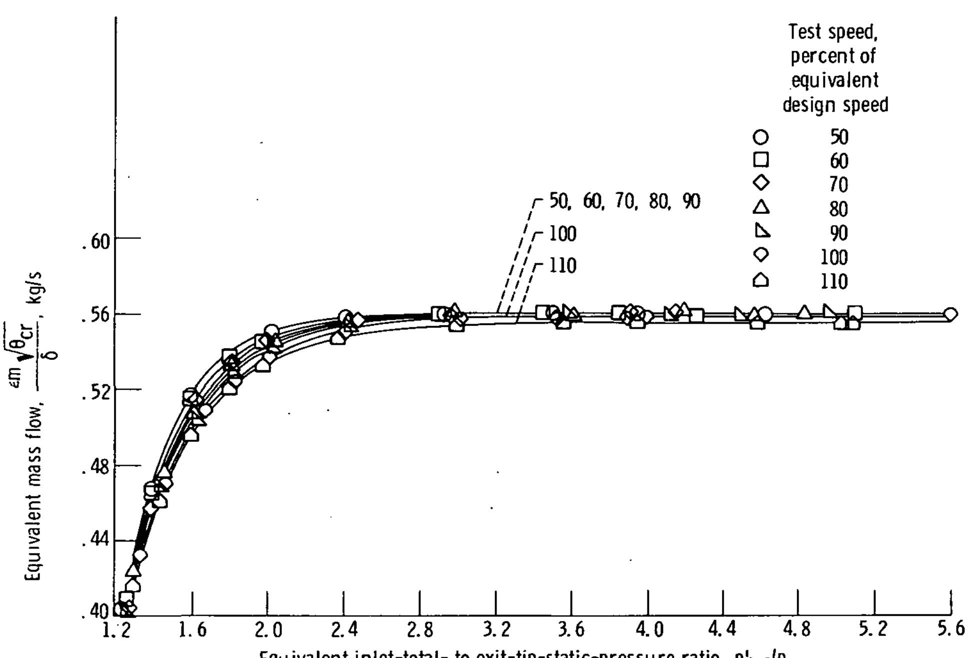

Figure 6. - Variation of equivalent mass flow with pressure ratio and speed.

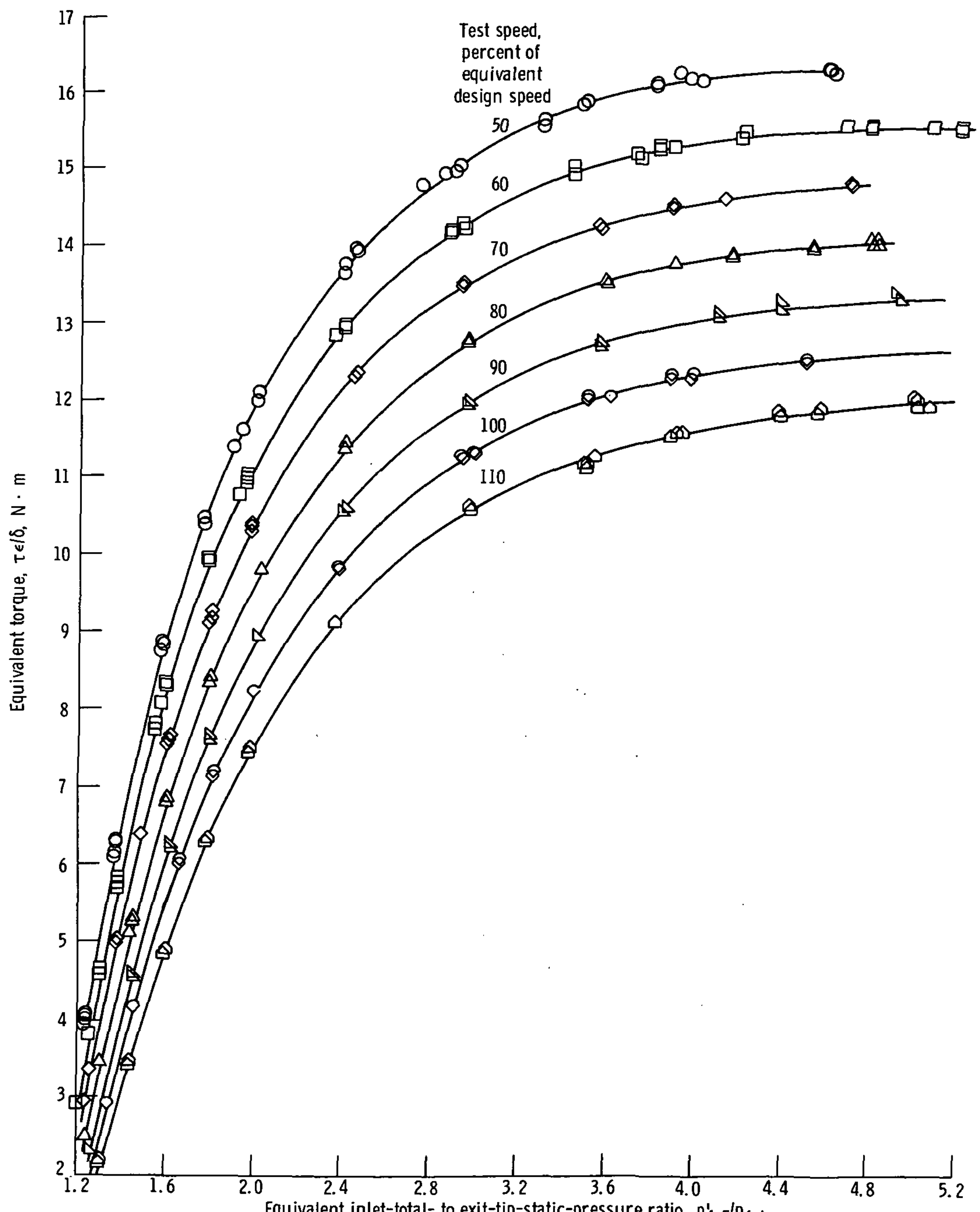

Figure 7. - Variation of torque with pressure ratio and speed.

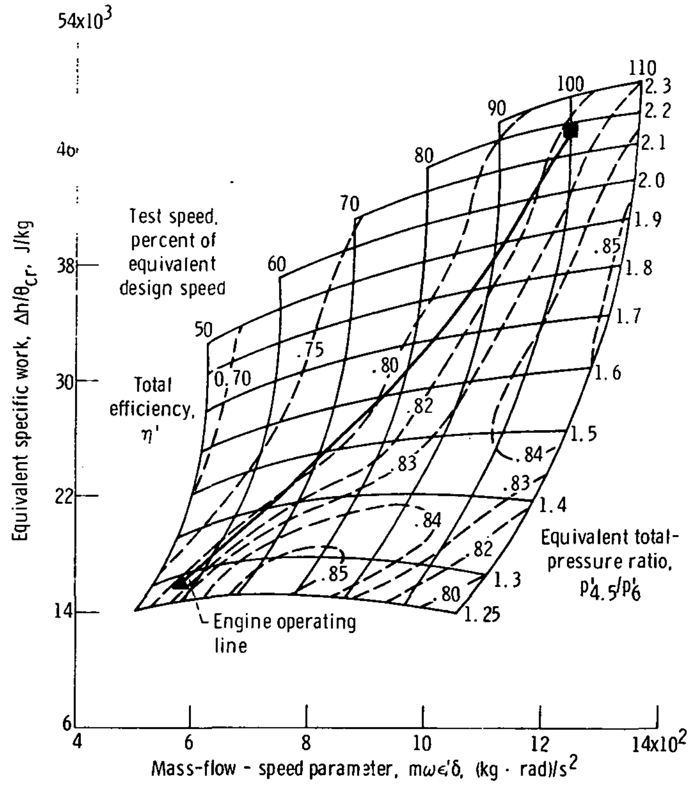

Figure 8. - Baseline compressor-drive-turbine performance map.

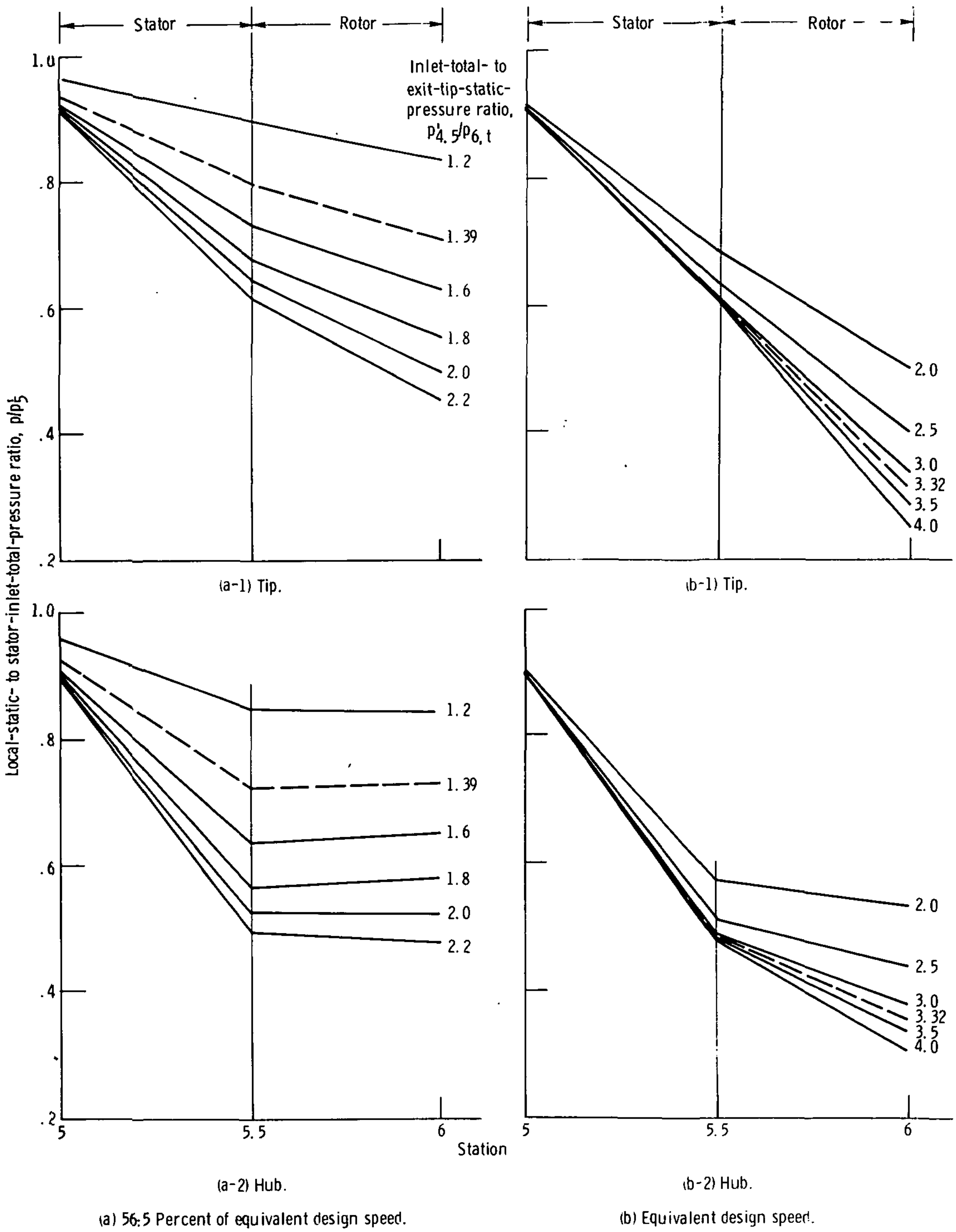

Figure 9. - Variation of static pressure through turbine for two speeds.

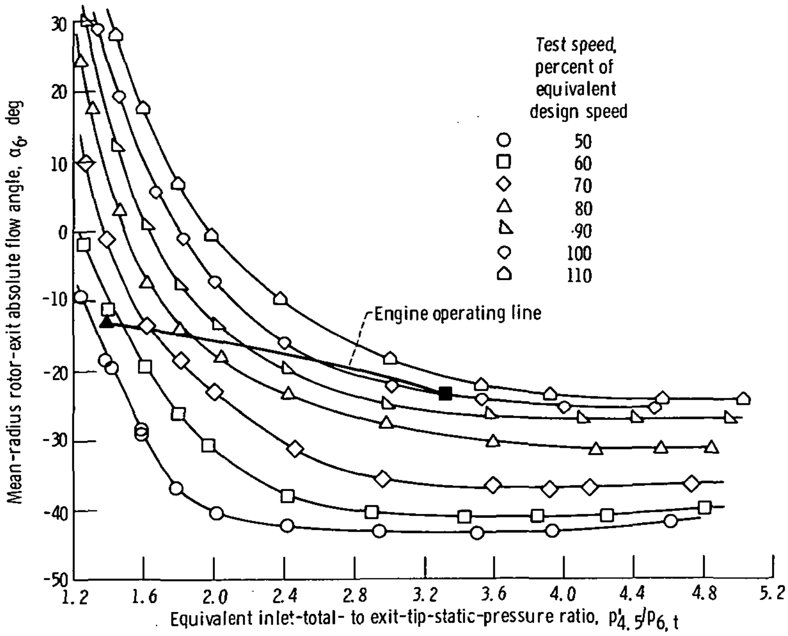

Figure 10. - Variation of mean-radius absolute flow angle at rotor exit with pressure ratio and speed.

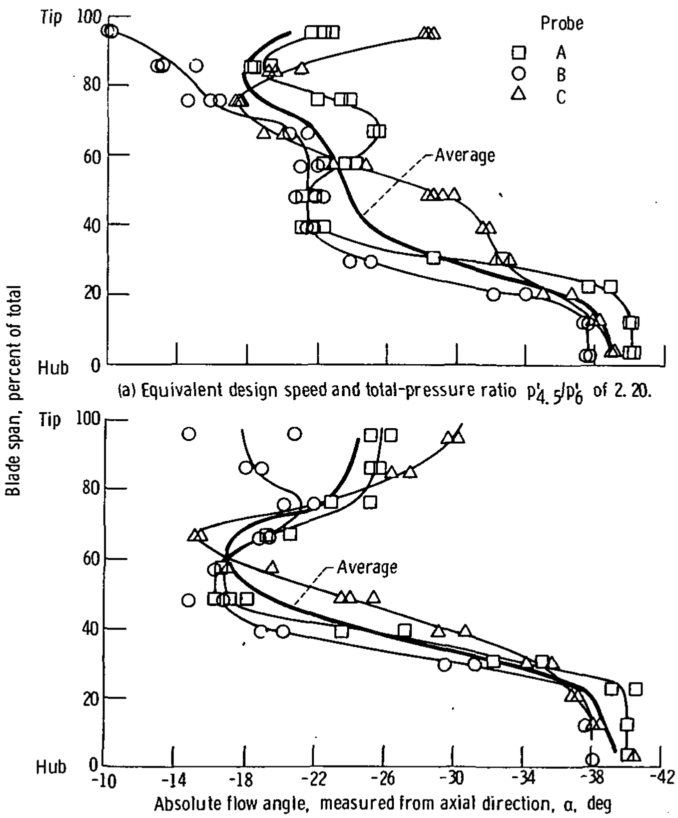

(a) Equivalent design speed and total-pressure ratio $p'_{4.5}/p'_6$ of 2.20.

(b) 51 Percent of equivalent design speed and total-pressure ratio $p'_{4.5}/p'_6$ of 1.31.

Figure 11. - Turbine-exit survey of absolute flow angle.

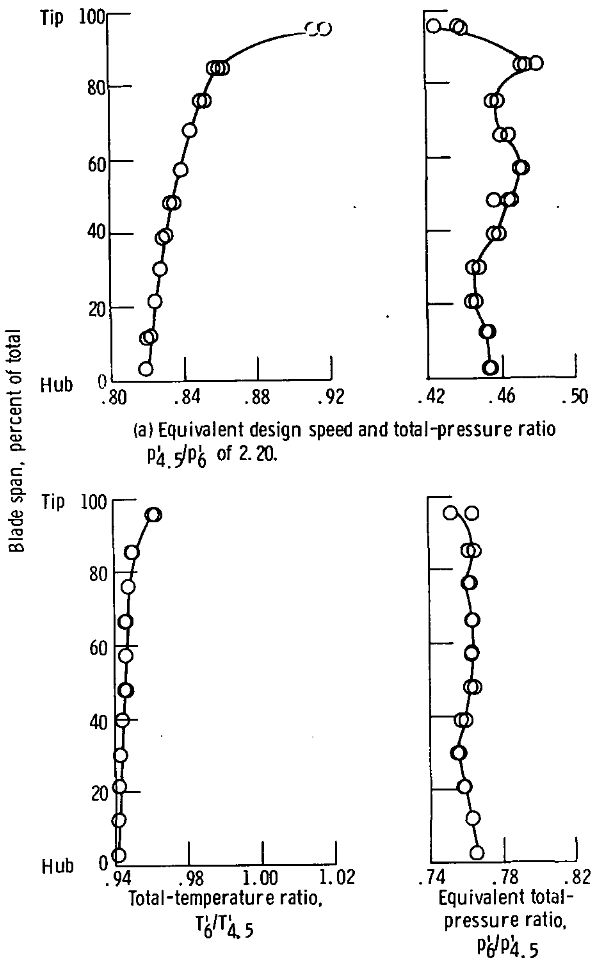

(a) Equivalent design speed and total-pressure ratio $p'_{4.5}/p'_6$ of 2.20.

(b) 51 Percent of equivalent design speed and total-pressure ratio $p'_{4.5}/p'_6$ of 1.31.

Figure 12. - Turbine-exit survey of total temperature and total pressure.

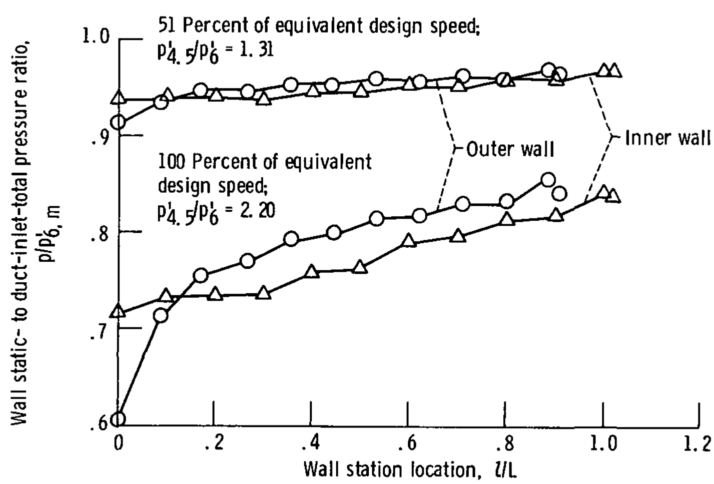

Figure 13. - Wall static pressures in transition duct.

1. Report No. NASA TM-78894	2. Government Accession No.	3. Recipient's Catalog No.
4. Title and Subtitle COLD-AIR PERFORMANCE OF THE COMPRESSOR-DRIVE TURBINE OF THE DEPARTMENT OF ENERGY BASELINE AUTOMOBILE GAS-TURBINE ENGINE		5. Report Date July 1978
		6. Performing Organization Code
7. Author(s) Richard J. Roelke and Kerry L. McLallin		8. Performing Organization Report No. E-9480
		10. Work Unit No.
9. Performing Organization Name and Address National Aeronautics and Space Administration Lewis Research Center Cleveland, Ohio 44135		11. Contract or Grant No.
		13. Type of Report and Period Covered Technical Memorandum
12. Sponsoring Agency Name and Address U.S. Department of Energy Division of Transportation Energy Conservation Washington, D.C. 20545		14. Sponsoring Agency ~~Code~~ Report No. DOE/NASA/1011-78/25

15. Supplementary Notes

Final report. Prepared under Interagency Agreement EC-77-A-31-1011.

16. Abstract

The aerodynamic performance of the compressor-drive turbine of the DOE baseline gas-turbine engine was determined over a range of pressure ratios and speeds. In addition, static pressures were measured in the diffusing transition duct located immediately downstream of the turbine. Results are presented in terms of mass flow, torque, specific work, and efficiency for the turbine and in terms of pressure recovery and effectiveness for the transition duct.

17. Key Words (Suggested by Author(s))	18. Distribution Statement
Automobile engines Turbine engines Performance tests	Unclassified - unlimited STAR Category 02 DOE Category UC-96

19. Security Classif. (of this report)	20. Security Classif. (of this page)	21. No. of Pages	22. Price*
Unclassified	Unclassified	22	A02

* For sale by the National Technical Information Service, Springfield, Virginia 22161

NASA-Langley, 1978

National Aeronautics and
Space Administration

Washington, D.C.
20546

SPECIAL FOURTH CLASS MAIL
BOOK

Postage and Fees Paid
National Aeronautics and
Space Administration
NASA-451

U.S.MAIL

7 2 1U,A, 053078 S90844HU
MCDONNELL DOUGLAS CORP
ATTN: PUBLICATIONS GROUP PR 15246-A
P O BOX 516
ST LOUIS MO 63166

NASA

POSTMASTER: If Undeliverable (Section 158
Postal Manual) Do Not Return

7 SEP 78 R. Wieckmann 342/32²/260/23579 8 SEP 78

6 JUN 80 Jim Orgorouski 210 32 210 23330

NOV 1993